Lasers in Manufacturing Conference 2015

Laser Power Modulation to Minimize the Electrical Resistance of Aluminum-Copper Welds

Florian Fetzer[a]*, M. Jarwitz[a], P. Stritt[a], R. Weber[a], T. Graf[a]

[a]*Institut für Strahlwerkzeuge, Pfaffenwaldring 43, 70569 Stuttgart, Germany*

Abstract

Power modulated overlap-welding of Cu-OF to Al99.5 was investigated with the aim of minimizing the welds electrical resistance. In-situ X-ray videography was used to measure the intrusion depth of copper into the aluminum sheet with acquisition rates of up to 5 kHz. Temperatures in the weld pool were measured synchronously and a concurrence of both signals is found. It is shown that laser power modulation at frequencies from 100 Hz to 400 Hz can increase the process stability, whereas its influence on the electrical resistance of the joints is negligible. Beside, an influence of the top material on this resistance was found and we claim the aluminum-top configuration to be superior.

Keywords: Laser welding, diagnostics, dissimilar metals, electrical resistivity ;

1. Introduction

Joining of copper to aluminum is of interest in a growing range of seminal applications, such as e-mobility and light weight construction, as shown by Kirchhoff, 2013. Laser welding is one of the favorable joining technologies regarding productivity. Laser welding of dissimilar metals, however, involves the formation of brittle intermetallic phases. These degrade the mechanical and electrical properties of the welds as Braunovic and Alexandrov, 1994, and Rabkin and Ryabov, 1970 elaborate, the latter being the critical factor in most applications of copper-aluminum joints. While the laser welding of the pure materials aluminum and copper is challenging well enough, as Dausinger and Rapp, 1996 and Hess and Schuster, 2011 show, the

* Corresponding author. Tel.: +49(0)711 685-66868.
E-mail address: florian.fetzer@ifsw.uni.stuttgart.de

complexity of joining the two metals is boosted by the materials diverse properties and low solubility. To gain a comprehensive understanding of the welding process, online X-ray videography can be applied, well recognized for in-situ analysis of the melt pool shape, keyhole geometry and defect creation as Abt and Boley, 2011, Boley and Abt, 2013, Heider and Boley and Rominger et al., 2012 showed. Pyrometric measurements allow for temporally highly resolved measurements of the weld pool temperature and its gradient, as applied by Jarwitz and Stritt, 2014. We applied both approaches to investigate the influence of laser power modulation on the process stability and on the electrical resistance of the dissimilar materials welds.

2. Experimental Setup

Electronic grade oxygen-free copper (Cu-OF) and high-purity aluminum (Al99.5) sheets were laser welded in overlap configuration. The experiments were performed using a solid state laser at a wavelength of 1.085 µm. The focal diameter was 260 µm with a Rayleigh-length of 6 mm, focused on the surface of the upper sheet. To avoid detrimental back reflection, the laser optics was inclined with an angle of 10° in welding direction. The experiments were performed using two slightly varying setups.

2.1. Welding process diagnostics

For a first series of experiments samples of 5 mm width, 1 mm height and 100 mm length were used to allow for high speed in-situ X-ray videography. The X-ray radiation, generated at an electron acceleration voltage of 60 kV, was irradiating the sample orthogonally to the plane defined by the laser beam propagation axis and the direction of the sample movement. A scintillator converted the transmitted X-rays into visual light and a succeeding image amplifier was recorded by a high speed camera with up to 5 kHz framerate. The weld pool temperature was measured 1 mm and 2 mm behind the keyhole using two Dr. Mergenthaler GmbH & Co. KG LASCON® pyrometers operated in single band measurement mode. The spot diameters for this temperature probing were 400 µm and measurements were performed at an acquisition rate of 10 kHz. The emissivity was set to that of the top material, $\epsilon_{cu} = 0.07$ for copper, as proposed by Watanabe and Susa, 2003. Additionally, the weld pool dynamics was recorded with a high speed camera from top view at 5 kHz framerate.

2.2. Electrical resistance measurements

In a second series of experiments the effects on the electrical resistance of the welds were measured. Therefore sheets of 45 mm width, 1 mm height and 100 mm length were joined with welds of 35 mm length centered in the 30 mm wide overlapping area. The welding parameters were identical.

Four-point measurements were performed on the samples from series 2 to obtain reproducible measurements of the electrical resistance. A controlled constant current, I_{set}, was applied from one sheet through the joint to a contact point at the second sheet. The distance between these contacts was 40 mm. Using an independent circuit, a nano-voltmeter probed the voltage drop, U_j, between the two contact points over the weld. To level thermal potentials due to the metal interfaces, the direction of the current was switched 100 times during one metering process and for each of these currents the voltage was measured. The resultant resistance is calculated as

$$R = \sum_{j=0}^{N-2} \frac{U_j - 2U_{j+1} + U_{j+2}}{4I_{set}}, \qquad (1)$$

containing the parts through pure copper (over the distance x_1) and through pure aluminum (x_2) on both sides of the weld. To determine this effect and to quantify the sole resistance of the weld, a series of measurements was performed, where the two measurement tips probing U were gradually shifted from the copper to the aluminum side. Thus x_1 and x_2 were changed but the overall distance of $x_1 + x_2 = 40$ mm remained constant. As pictured in Fig. 1 the acquired resistance values were found to be linearly dependent on the difference between x_1 and x_2. A linear fit results in a line parallel shifted to the theoretically calculated resistances using the specific resistances of pure copper ($0.01721\,\Omega/mm^2 \cdot m$) and pure aluminum ($0.0265\,\Omega/mm^2 \cdot m$). The evaluated measurements were corrected for the vertical offset of 21 µΩ, resulting from the resistance of the pure metals over the distances x_1 and x_2 , respectively.

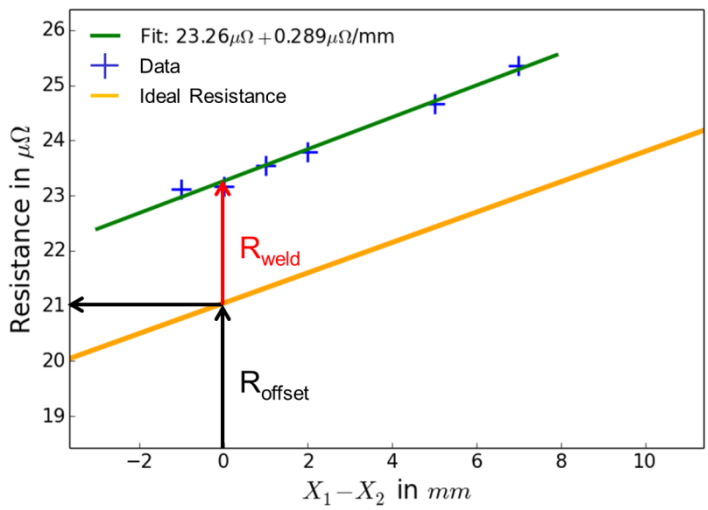

Fig. 1. The voltage drop between the two contact points in dependence of the joint position (blue markers). The parallel shifted orange line represents the expected values given perfect connection between the two sheets.

A potential uneven positioning of $x_1 - x_2 = a \neq 0$ was taken into account by flipping the samples in the positioning device for a second measurement, resulting in $x_1 - x_2 = -a \neq 0$. Averaging both measurements led to in total equal distances through both materials for the current to pass.

2.3. Evaluation of the X-ray videos

Due to the difference in density and proton number the X-ray attenuation in copper exceeds that of aluminum. Assuming an exponential attenuation of the radiation when passing d mm of absorbing material as

$$I(d) = I_0 \cdot e^{-\gamma \cdot d}, \qquad (2)$$

we measured $\gamma_{cu} = 2.63/mm$ for copper and $\gamma_{al} = 0.167/mm$ for aluminum at our setup. This difference allows identifying the penetration of copper into the aluminum in the X-ray images. A single frame out of the synchronized high speed videos of the weld seam (top) and the X-ray video (bottom) is depicted in Fig. 2. The red circles indicate the positions of the temperature measurements. The copper sheet in the upper part of the image almost completely absorbs the X-ray radiation, resulting in the black image region. In the lower part the mixing of the strongly absorbing copper into the aluminum is visible. This fact was used to evaluate the X-ray videos with respect to the mixing depth of copper into aluminum. Therefore, every frame was scaled for the effective X-ray intensity measured in a reference region of the images, to take fluctuations of the X-ray tube into account. Additionally, a spatial mean filter was applied to lower the influence of noise. A threshold of pixel intensity, which defined the lower limit for mapping a pixel to pure aluminum, was defined. This threshold was calibrated by longitudinal sections and Energy-dispersive X-ray spectroscopy (EDX) measurements. It was set to the 70th percentile of pixel values in the X-ray images. Fig. 2 (b) shows the processed X-ray frame of (a) in that same figure. The pixels mapped to aluminum are displayed in white and those corresponding to copper or a materials mixture in black. The vertical position of the black-white interface was defined as the penetration depth of the copper into aluminum.

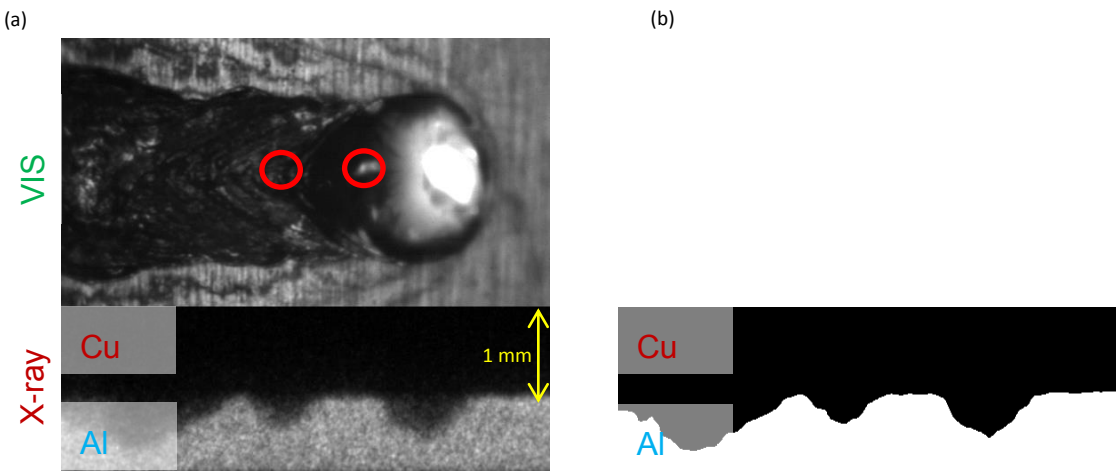

Fig. 2. Welding of copper onto aluminum at 3.5 kW and 9 m/min federate. (a) Concurrent single frames from high speed videos of the weld seam in top view (upper picture) and the X-ray video (bottom). (b) Processed frame used for depth evaluation.

In Fig. 3 a longitudinal section used for the threshold calibration of the depth evaluation is shown. The blue curve indicates the penetration depth as measured from the corresponding X-ray video. The red line

shows the temperatures measured at position 1. We note a significant coherence of the two signals, indicating that an increased temperature is measured when the penetraition depth of the copper in aluminum increases.

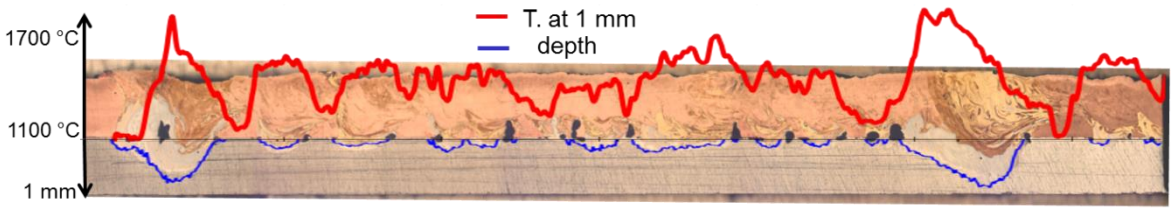

Fig. 3. Longitudinal section of the cw 3.5 kW, 9 m/min process. The blue curve indicates the depth signal evaluated from the corresponding X-ray video. The red curve schematically depicts the temperatures measured 1 mm behind the keyhole to visualize the concurrence of the two signals.

3. Experimental results

3.1. Process instabilities in cw welds

As typically seen in Fig. 3 for cw welded copper-aluminum joints process sections, where no fusing of the aluminum occurs, alternate with such where the lower sheet is fully penetrated and the materials mix over the total depth. For feed rates from 5 m/min to 10 m/min we measured the average penetration depth as

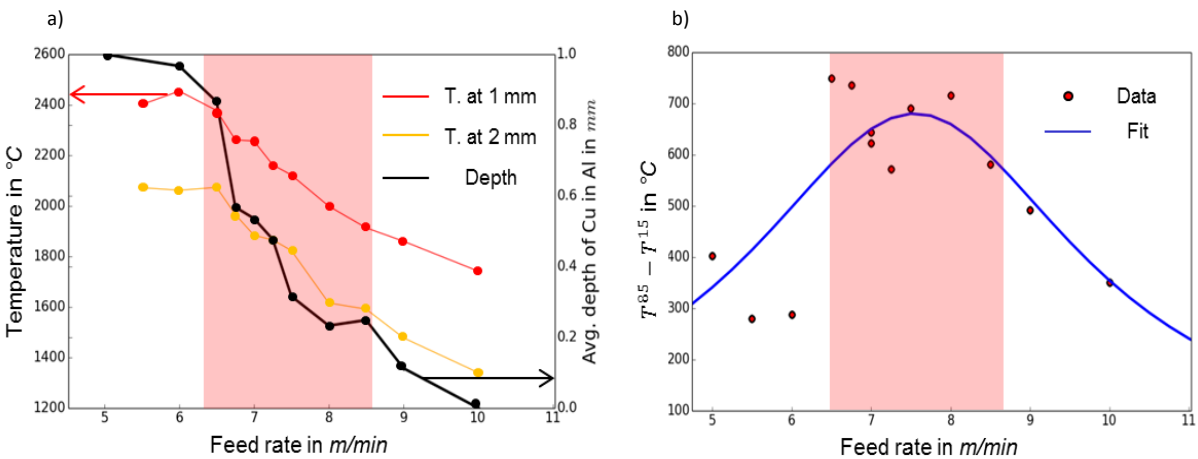

Fig. 4. (a) The black curve (right scale) shows the average intrusion depth over feed rate, while the red and orange curves represent the average of the metered temperature 1 mm and 2 mm behind the keyhole. (b) Process instability in dependence of the feed rate for 3.25 kW laser power. The blue curve shows the Lorentzian fit through these data points. The average laser power was 3.25 kW.

described before and the average temperature at 1 mm and 2 mm behind the keyhole, as shown in Fig. 4 (a). Strong concurrence between the temperature measured on the weld pools surface and the intrusion depth of copper is found. When welding with laser power of 3.25 kW within a feed rate range from 6 m/min to 9 m/min (the red marked regime in Fig. 4) a stable welding depth could not be achieved. The

observed processes were unstable and switch between both extremes, which manifests itself in the depth, as well as in the strongly fluctuating temperature signal. In order to quantify these instabilities, we determined the fluctuation of the temperature signals. As a measure for this property the difference between the 85th and the 15th percentile of the measured temperatures was taken. Fig. 4 (b) shows the result for the temperature at the 1 mm position, the blue curve representing a Lorentzian fit through the data points to guide the eye. Throughout the range of neither constant full, nor zero penetration the measured temperature oscillations are most intense. Although there is a cw power input into the process, the measured output – in terms of temperature and depth – is highly fluctuating.

3.2. Laser power modulation

3.2.1 Influence on depth fluctuations

In case of welding pure copper power modulation was found to increase the welds quality in terms of stability and defects by Heider and Stritt, 2011. Also in case of dissimilar metal welding, pulse shape forming has been applied to affect the welds metallurgy, as shown in Stritt and Hagenlocher, 2014.

Two parameter series were investigated: 1) welding with a feed rate of 9 m/min at an average power of 3.5 kW. In cw welding these process parameters yielded the most stable welds. 2) A feed rate of 7 m/min and 3.25 kW average power, which showed the most intense depth fluctuations in cw welding. Sinusoidal laser power modulations with frequencies up to 800 Hz were applied. The amplitude of the modulation was 500 W. For every parameter we measured the time resolved penetration depth $d(t)$ using the X-ray analysis as described before. As a measure for the instability of this depth its variance $\sigma^2(d)$ was determined. The left scale of Fig. 5 shows the measured values for both parameter series in dependence of the modulation frequency. For 50 Hz the process almost entirely follows the laser power. At this frequency the spatial distance over one modulation period larger than the weld pool length as measured from the high speed videos. An interchange between full- and zero penetration is observed which obeys the input frequency.

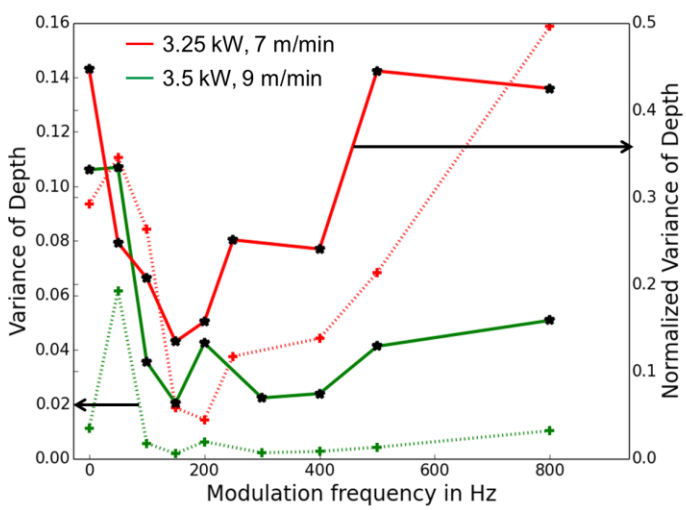

Fig. 5. Process instabilities in dependence of power modulation frequency. The green curves represent the process at 3.5 kW and 9 m/min feed rate, the red curve 3.25 kW and 7 m/min.

In the range from 100 Hz to 400 Hz we measure the most stable processes in terms of variance of penetration depth. For higher frequencies the process approximates the cw case. At 50 Hz modulation frequency the calculated variance is higher than in the corresponding cw process for both series. However, at this frequency also the average penetration depth is higher. To take a frequency dependent penetration depth into account, the normalized variance, $\sigma^2(d)/\bar{d}$, (right scale of Fig. 5) was measured. Here $\bar{d}$ denotes the average of the depth signal. This reveals the fact, that relative to average welding depth, the cw process fluctuates at least as strong as the corresponding, for 500 W and 50 Hz, modulated process. Moreover, in the cw case, these fluctuations happen in an uncontrolled manner. In contrast, if laser power modulation is applied, the depth fluctuations mostly follow the laser power.

3.2.1 Influence on electrical resistance

Sample geometry 2 was used to perform measurements of the electrical resistance. We compared the two parameter sets described in the previous section and additionally two series with aluminum as top material. The parameters in the aluminum-top configuration were 1.75 kW and 1.3 kW of average laser power at 6 m/min feed rate. This resulted in similar average welding depths as in the case of the copper-top configurations. Fig. 6 pictures the obtained data, comparing the four configurations. The two copper-top configurations yielded significantly higher resistance values throughout all applied modulation frequencies. Averaged over all measurements, the 3.25 kW – 7 m/min process, which performed worst, resulted in a 60% higher electrical resistivity than the 1.75 kW – 6 m/min process in aluminum- top configuration.

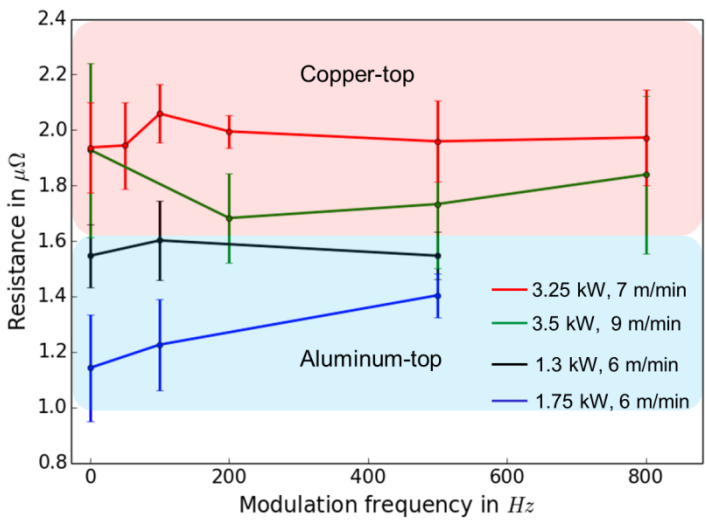

Fig. 6. Electrical resistance of the welds. The measured values are corrected for the electrical resistance of the pure material aside the joints.

Despite the fact that the fluctuations of the penetration depth could be suppressed by power modulation, no significant dependence of the electrical resistance on the modulation frequency was found.

4. Conclusion

Laser welding of copper to aluminum in overlap configuration was investigated by in-situ X-Ray videography and pyrometric temperature measurements. The temperatures measured on the melt pool surface cohere with the measured penetration depth of copper into the aluminum sheet, as calculated from the X-ray videos. The copper-top configuration shows inherent instabilities when the copper intrudes the lower aluminum sheet. Laser power modulation with frequencies in the range from 100 Hz to 400 Hz stabilizes the fluctuations of the penetration depth. The comparison of the electrical resistance measurements and the process diagnostics leads to the conclusion, that a laser power modulation at these frequencies stabilizes the process without negative influence on the welds metallurgical and electrical properties.

Acknowledgements

The presented work was funded by the Federal Ministry of Education and Research (BMBF) and the experiments were done in the context of the “ReMiLas” project. The responsibility for this paper is taken by the authors.

References

Kirchhoff, M., 2013. Laser applications in battery production — From cutting foils to welding the case: Proceedings October 29th-30th, 2013, Nuremberg, Germany, 2013.

Braunovic, M. and Alexandrov, N., 1994. Intermetallic compounds at aluminum-to-copper electrical interfaces: effect of temperature and electric current, IEEE Trans. Comp., Packag., Manufact. Technol. A, 17, 78–85, doi:10.1109/95.296372, 1994.

Dausinger, F., Rapp, J., Beck, M., Faisst, F., Hack, R., and Hügel, H., 1996. Welding of aluminum: A challenging opportunity for laser technology, J. Laser Appl., 8, 285, doi:10.2351/1.4745434, 1996.

Hess, A., Schuster, R., Heider, A., Weber, R., and Graf, T., 2011. Continuous Wave Laser Welding of Copper with Combined Beams at Wavelengths of 1030nm and of 515nm, Physics Procedia, 12, 88–94, doi:10.1016/j.phpro.2011.03.012, 2011.

Abt, F., Boley, M., Weber, R., Graf, T., Popko, G., and Nau, S., 2011. Novel X-ray System for in-situ Diagnostics of Laser Based Processes – First Experimental Results, Physics Procedia, 12, 761–770, doi:10.1016/j.phpro.2011.03.095, 2011.

Boley, M., Abt, F., Weber, R., and Graf, T., 2013. X-Ray and Optical Videography for 3D Measurement of Capillary and Melt Pool Geometry in Laser Welding, Physics Procedia, 41, 488–495, doi:10.1016/j.phpro.2013.03.105, 2013.

Heider, A., Boley, M., Weber, R., and Graf, T. Investigation of Spatter Formation in Laser Welding of Copper using High - Speed Online X - Ray Imaging, LAMP 2013, 2013.

Rominger, V. et al., 2012. FORMATION MECHANISM OF PROCESS INSTABILITIES AND STRATEGIES TO IMPROVE WELDING QUALITY, 31th International Congress on Applications of Lasers & Electro-Optics, 2012.

Jarwitz, M., Stritt, P., Weber, R., and Graf, T., 2014. TEMPORALLY RESOLVED MEASUREMENT OF TEMPERATURE GRADIENTS DURING POWER MODULATED LASER WELDING OF COPPER TO ALUMINUM, 33rd International congress on applications of lasers & electro-optics (ICALEO), 19.-23.10. 2014, San Diego, USA, 2014.

Watanabe, H., Susa, M., Fukuyama, H., and Nagata, K., 2003. Near-Infrared Spectral Emissivity of Cu, Ag, and Au in the Liquid and Solid States at Their Melting Points, International Journal of Thermophysics, 24, 1105–1120, doi:10.1023/A:1025013320127, 2003.

Bautze, T. and Kogel-Hollacher, M., 2014. Keyhole Depth is just a Distance, LTJ, 11, 39–43, doi:10.1002/latj.201400040, 2014.

Heider, A., Stritt, P., Hess, A., Weber, R., and Graf, T., 2011. Process Stabilization at welding Copper by Laser Power Modulation, Physics Procedia, 12, 81–87, doi:10.1016/j.phpro.2011.03.011, 2011.

Stritt, P., Hagenlocher, C., Kizler, C., Weber, R., Rüttimann, C., and Graf, T., 2014. Laser Spot Welding of Copper-aluminum Joints Using a Pulsed Dual Wavelength Laser at 532 and 1064nm, Physics Procedia, 56, 759–767, doi:10.1016/j.phpro.2014.08.083, 2014.

Rabkin, D. M., Ryabov, V. R., Lozovskaya, A. V., and Dovzhenko, V. A., 1970. Preparation and properties of copper-aluminum intermetallic compounds, Powder Metall Met Ceram, 9, 695–700, doi:10.1007/BF00803820, 1970.